WILEY

Biotechnology and Bioengineering

Biofilm growth of Chlorella sorokiniana in a rotating biological contactor based photobioreactor

Journal:	*Biotechnology and Bioengineering*
Manuscript ID:	14-109.R1
Wiley - Manuscript type:	Article
Date Submitted by the Author:	29-Apr-2014
Complete List of Authors:	Blanken, Ward; Wageningen University, Bioprocess Engineering, AlgaePARC Janssen, Marcel; Wageningen University, Bioprocess Engineering, AlgaePARC Cuaresma, Maria; Wageningen University, Bioprocess Engineering; University of Huelva, Chemistry and Material Sciences Bhaiji, Tasneem; Cranfield University, Manufacturing and Materials Department Libor, Zsuzsanna; Cranfield University, Manufacturing and Materials Department Wijffels, Rene; Wageningen University, Bioprocess Engineering, AlgaePARC
Key Words:	Biofilm, photobioreactor, Chlorella, productivity, substratum , microalgae

Biofilm growth of *Chlorella sorokiniana* in a rotating biological contactor based photobioreactor

W. Blanken[a,1], M. Janssen[a,2], M. Cuaresma[a,b], Z. Libor[c], T. Bhaiji[c], R.H. Wijffels[a],

[a] Bioprocess Engineering, AlgaePARC, Wageningen University, PO Box 8129, 6700 EV, Wageningen, The Netherlands,www.AlgaePARC.com

[b] Algal Biotechnology Group, International Centre for Environmental Research (Ciecem), University of Huelva, ParqueDunar s/n, Matalascañas, Almonte, 21760 Huelva, Spain

[c] Manufacturing and Materials Department, School of Applied Sciences, Cranfield University, Collage Road, Cranfield, MK43 0AL, United Kingdom, www.cranfield.ac.uk

[1] Corresponding author. Tel.: + 31 317 483 595. Email: ward.blanken@wur.nl;

[2] Corresponding author. Tel.: + 31 317 484 708. Email: marcel.janssen@wur.nl;

Abstract

Microalgae biofilms could be used as a production platform for microalgae biomass. In this study, a photobioreactor design based on a rotating biological contactor (RBC) was used as a production platform for microalgae biomass cultivated in biofilm. In the photobioreactor, referred to as Algadisk, microalgae grow in biofilm on vertical rotating disks partially submerged in a growth medium. The objective is to evaluate the potential of the Algadisk photobioreactor with respect to the effects of disk roughness, disk rotation speed and CO_2 concentration. These objectives where evaluated in relationship to productivity, photosynthetic efficiency, and long-term cultivation stability in a lab-scale Algadisk system. Although the lab-scale Algadisk system is used, operation parameters evaluated are relevant for scale-up.

Chlorella Sorokiniana was used as model microalgae. In the lab-scale Algadisk reactor, productivity of 20.1 ±0.7 gram per m^2 disk surface per day and a biomass yield on light of 0.9 ±0.04 grams dry weight biomass per mol photons were obtained. Different disk rotation speeds did demonstrate minimal effects on biofilm growth and on the diffusion of substrate into the biofilm. CO_2 limitation, however, drastically reduced productivity to 2-4 gram per m^2 disk surface per day. Productivity could be maintained over a period of 21 weeks without re-inoculation of the Algadisk. Productivity decreased under extreme conditions such as pH 9-10, temperature above 40ºC, and with low CO_2 concentrations. Maximal productivity, however, was promptly recovered when optimal cultivation conditions were reinstated. These results exhibit an apparent opportunity to employ the Algadisk photobioreactor at large scale for microalgae biomass production if diffusion does not limit the CO_2 supply.

1 Introduction

Biofilm-photobioreactors can turn the problem of biofilm formation on the walls of suspended photobioreactors (Jacobsen et al. 2010) into an opportunity. Biofilm-photobioreactors pose several advantages over suspended cultivation of microalgae including the harvest of high dry solid content, a decreased energy requirement (Ozkan et al. 2012), and the possibility of operating at short hydraulic retention times without wash out of the microalgae (Patwardhan 2003). Disadvantages are the formation of gradients over the biofilm for pH, nutrients, and light (Wolf et al. 2007).

Biofilm-photobioreactors are increasingly attracting attention as a cultivation platform because of the advantages discussed above. Because of the possibility to operate at short hydraulic retention times biofilm-photobioreactors are widely studied as part of wastewater treatment. Wastewater treatment plants often operate to clean diluted waste streams at short hydraulic retention times (Patwardhan 2003). Biofilm photobioreactor designs that have been proposed for waste water treatment include rotating spools (Christenson and Sims 2012), rotating brushes (Wei et al. 2008), vertical sheets (Boelee et al. 2012), tubular flow cells (de Godos et al. 2009) and horizontal flow cells (Wilkie and Mulbry 2002). The main disadvantage most of the above systems share are limited control of microalgae species and low productivities. In recent years, a range of biofilm-photobioreactors were developed that intend to employ the biofilm growth as a controllable production platform of dedicated microalgal species. Examples include the twin layer system (Naumann et al. 2012; Nowack et al. 2005; Shi et al. 2007), a similar design referred to as an attached photobioreactor (Ji et al. 2013a; Ji et al. 2013b), the rotating spool system (Christenson and Sims 2012), and the rotating algal biofilm cultivation system (Gross et al. 2013).

In this study a biofilm photobioreactor based on the rotating biological contactor (RBC) design, the Algadisk system, was tested. RBC were exploited for aerobic wastewater treatment

(Patwardhan 2003), however a recent study evaluated the performance of a phototropic RBC to remove heavy metal from waste streams (Orandi et al. 2012). The four major advantages of the RBC design are (1) the lower ratio between footprint and cultivation surface compared to horizontal systems (Wijffels and Barbosa 2010); (2) the opportunity to regulate the average light intensity per disk by varying the disk size and distances between disks (Orandi et al. 2012); (3) that rotation ensures a simple but repetitive contact with the growth medium; and (4) efficient gas-biofilm mass transfer as a result of a large biofilm area exposed to the gas phase and short diffusion paths from gas to the biofilm. The enhanced gas-biofilm mass transfer saves energy since the energy intensive sparging of the culture broth might not be needed (Patwardhan 2003). However, two disadvantages of the RBC design include: (1) the influence of rotation speeds on biofilm performance, high rotation speeds will increase mass transfer and shear while slow rotation speeds will decrease mass transfer and might result in drying (Gross et al. 2013); (2) spatial separation of light and CO_2 from the dissolved nutrients, which could result in nutrient limitations. To test the Algadisk design, a lab-scale version was constructed. The objective is to evaluate the potential of the Algadisk photobioreactor with respect to the effects of disk roughness, disk rotation speed and CO_2 concentration. These objectives where evaluated in relationship to productivity, photosynthetic efficiency, and long-term cultivation stability in a lab-scale Algadisk system. Although the lab-scale Algadisk system is used, operation parameters evaluated are relevant for scale-up.

2 Materials and methods

2.1 Pre cultivation

The microalgae *Chlorella sorokiniana* (Sorokin and Myers 1953) was pre-cultivated in shake flasks with M8-a medium (Kliphuis et al. 2010). The algae suspension was used to inoculate the disks, as will be explained later. The M8-a media was supplemented with 30 mM Urea as nitrogen source, and pH was set to 6.7. In the reactor medium, an additional 8 mM $NaHCO_3$

was included after setting the pH to increase the dissolved CO_2 concentration. Anti-foam B (J.T.Baker, The Netherlands) was directly added to the culture broth in the event of foam formation. The M8-a medium contains all dissolved species in excess, therefore microalgae grow under nutrient-replete and light-limited conditions in our experiments.

2.2 Experimental set-up

The experimental setup consisted of a water tight container, four disks and eight lamps, (Figure 1). The container measured 1220*70*130 mm (L*W*H) and contained 11 L of the M8-a medium. The disks were located inside the water tight container with 42% of the disk surface submerged. The liquid volume in the container was kept constant via an overflow connected to a 10 L buffer tank (polycarbonate). The total volume of the system was 21 L. The temperature was measured and kept at 38 ±1 °C via a heat exchanger inside the buffer tank. The medium was circulated between the buffer tank and the container at a rate of 6 L min^{-1} (MD-6Z, Iwaki, Japan). The pH in the buffer tank was maintained between 6.7 and 6.8 by pulse-wise addition of CO_2 gas or HCl (see section 2.4). Liquid lost by evaporation was detected with a level sensor in the buffer tank and was automatically replaced by filtered tap water.

Both sides of the disks were illuminated by a warm-white directional LED light source (warm white 45mil chip, Bridgelux, USA). Since the open water container was not transparent, only the upper portion of the disks was illuminated. This strategy allowed for a selective pressure to stimulate biofilm growth while it minimized microalgae growth in the suspension. Inoculation was performed by adding a microalgae suspension pre-cultivated in a shake flask to the container with the culture media. The selective pressure for biofilm growth was used to initiate biofilm development. After the initial biofilm developed, the biofilm was harvested by scraping. After harvesting, the biofilm could re-grow from the biomass that remained on the disk surface. After the initial harvest (discussed in section 2.7), the biofilm was harvested every seventh day; this cycle is referred to as a 7 day growth-harvest cycle. An example of a typical 7 day growth-

harvest cycle is illustrated in Figure 2. After every growth-harvest cycle the reactor was cleaned and filled with fresh medium.

2.3 Disk rotation speeds

The rotation speed of the disks could be modified and is depicted in revolutions per minute (rpm). The actual rotation speed is provided for each experiment. However, only the rotation speeds 3, 6, 11, and 20 rpm were evaluated in this study. These speeds correlate to velocities over the disk radius ranging from 0.01 to 0.25 m s^{-1} (section 3.3). All disks were spun in the same direction as the liquid flow (0.01 m s^{-1}), assuming constant flow over the entire cross section. All rotation speeds were tested at all disk positions to exclude possible effects of positioning within the container.

2.4 CO_2 supply

Three CO_2 supply conditions were evaluated. The first condition is at nutrient-replete conditions. In all experiments at nutrient-replete conditions 8 mM of $NaHCO_3$ was added to increase the dissolved CO_2 concentration. During the cultivation the CO_2 concentration was controlled based on pH. When microalgae consumed CO_2 the pH increased. This pH increase is countered by CO_2 addition resulting in a constant total carbon concentration of 15 mol m^{-3}. The total carbon concentration is the sum of dissolved CO_2 and HCO_3. The second condition was obtained by using a continuous airflow via sparging the water, containing 0.5%$_{v/v}$ CO_2 corresponding to a total carbon concentration of 0.7 mol m^{-3} if in equilibrium with water. The pH was controlled by the addition of hydrochloric acid (1.5 M HCl in water). The third conditions was obtained by not sparging the liquid and, therefore, only atmospheric CO_2 from the surrounding air was available. The 0.04%$_{v/v}$ CO_2 present in the atmosphere corresponds to a total carbon concentration of 0.06 mol m^{-3} at equilibrium with water. The pH was controlled by HCL addition. For both CO_2 limiting conditions no additional $NaHCO_3$ was added.

2.5 Disk materials:

Three different disk materials were used during this study: two stainless steel woven meshes and one sanded polycarbonate disk. The first mesh is a Twilled Dutch Weave type 80/700 (GKD SolidWeave, Gemany) with a tread thickness of 0.10/0.076 mm and a particle pass size of 47 µm, referred to as rough mesh. The second mesh is a Twilled Dutch Weave type 200/1400 (GKD SolidWeave, Germany) with tread thickness of 0.071/0.041 mm and a particle pass size of 15 µm, referred to as smooth mesh. The metal meshes were clamped onto a solid stainless steel disk with a 268 mm diameter with a stainless steel ring. The stainless steel ring (i.e., the clamp) was 14 mm wide and 2 mm thick resulting in a biofilm growth area with a 240 mm diameter. In the centre of the disk, a plastic cylinder with a diameter of 50 mm attached the axel to the disk.

The polycarbonate (PC) disk was coated with a polyelectrolyte multilayer coating. Polyvinylpyrrolidone (PVP, 55 000 Mw) and Polyacrylic acid (PAA , Mw 1800) (Sigma Aldrich, USA) were used for this coating. PVP is a neutral polymer that becomes positively charged when dissolved in phosphate buffer (PBS), and PAA is polyanionic and is negatively charged when dissolved. Polyelectrolytes solutions for dip coating were prepared at a concentration of 1 mg/ml of the polymer dissolved in PBS buffer. The polycarbonate disk was first cleaned with 70% ethanol and deionised water. The PC disk was subsequently submerged into the polyelectrolyte solution (PVP) to ensure that its surface was entirely covered for 15 minutes. The disk was then rinsed twice with deionised water and dried with nitrogen gas at room temperature and submerged into the oppositely charged polyelectrolyte (PAA) for 15 minutes followed by the same washing and drying procedure described above. This was repeated until the desired number of layers (PVP/PAA/PVP/PAA/PVP) was achieved. The PC disk was then placed under UV light for approximately 4 hours. The PC disk has the same growth area as the metal meshes.

The pore depth of the two metal meshes and the polycarbonate disk were compared. For the two steel meshes, the pore depth could be estimated based on CSLM analysis. From the CSLM analysis, it was determined that the rough mesh exhibited a maximal pore depth of 140 µm, and the fine mesh featured a maximal pore depth of 80 µm. To determine the structure on the hand sanded polycarbonate disk, a Dektak stylus profiler (Veeco, USA) was utilized. From the Dektak analysis over 2 mm, it was ascertained that the groves were, on average, 1 µm deep with a maximal depth of 10 µm.

2.6 Light measurement

The average light intensity over the illuminated disk surface was individually measured for every side of the disks. The light intensity was measured with a LI-COR 190-SA 2π quantum sensor (PAR range 400-700 nm) employing a template with 11 evenly spaced measure positions diffused over the disk surface as displayed in Appendix A. The average light intensity over all disk surfaces was 422 µmol $(m^2\ s)^{-1}$.

2.7 Harvest

Harvesting was performed by scraping as much biomass as possible from the disk surface with a metal scraper. The total weight of the collected wet biomass was measured, i.e. the wet biofilm weight. Afterwards, the biomass was dried overnight in an oven at 105 °C and weighed again, i.e. the dry biomass weight. By dividing the dry biomass weight with the wet biofilm weight, the mass fraction of biomass to water in the wet biofilm ($f_{x/w}$) was obtained (unit g/g).

2.8 Calculations

The surface productivity (P_x) in units g $(m^2\ d)^{-1}$ was calculated according to equation 1 with the total harvested dry weight (M_d) in g, the growth-harvest cycle time (t) in days, and disk surface (A_d) in m^2.

Equation 1, $$P_X = \frac{M_d}{t \cdot A_d}$$

The biomass yield on light ($Y_{X/ph}$) in g mol^{-1} was calculated according to equation 2 with incident light intensity (I_{in}) in mol $(m^2\ d)^{-1}$. The incident light is specific for every disk side and is compensated for the illuminated fraction above the water phase. The illuminated fraction of the disk is 58% [see Appendix A].

Equation 2, $$Y_{X/e} = \frac{P_x}{I_{in}}$$

The biofilm thickness (z) in m was calculated based on an estimated biofilm density (ρ_b) in kg m^{-3} (equations 3 and 4). The ρ_b is based on the assumption that water has a density (ρ_w) of 1000 kg m^{-3} and that the biomass has a density (ρ_X) of 1029 kg m^{-3} (Salim et al. 2013). The calculation of the mass fraction of biomass to water ($f_{x/w}$) was explained in section 2.7.

Equation 3, $$\rho_b = \left(f_{x/w} \cdot \rho_X\right) + \left(\left(1 - f_{x/w}\right) \cdot \rho_w\right)$$

Equation 4, $$z = \frac{M_d}{\rho_b \cdot A_d}$$

Standard deviations were calculated according to equation 5, with the individual measurements (x) (one 7 day growth-harvest cycle for one side of a disk)), the mean of all measurements ($\bar{x}$), and the number of measurements (n). The standard deviation of the areal productivity was calculated based on the variance in the measured areal productivities. All other Standard deviations were based on the rules of error propagation.

Equation 5, $$\sqrt{\frac{\sum(x-\bar{x})}{(n-1)}}$$

All p-values were calculated using an unpaired t-test.

3 Results

3.1 Evaluation of different disk materials

This experiment was performed to assess the influence of disk material on the biofilm growth rate. To compare the two metal meshes and the polycarbonate disk, we performed an experiment at 422 µmol $(m^2\ s)^{-1}$, constant rotation speed of 11 rpm, and nutrient- and CO_2

replete conditions. A biofilm formed on the disks within 10 days following the inoculation of the medium with a microalgae suspension (optical density of 0.03 at 750 nm after inoculation). The productivity in the experiment's start-up phase was much less compared to the productivity of the subsequent growth-harvest cycles. Therefore, the start-up phase was not included in the presented data. Following the first harvest, four growth-harvest cycles were performed (n=8 as both sides are measured individually). The rough mesh productivity of 20.7 ±1.3 g $(m^2\ d)^{-1}$ was greater compared to both the productivity of 18.0 ±1.6 g $(m^2\ d)^{-1}$ of the fine mesh (p=0.002) and the 14.8±4.9 g $(m^2\ d)^{-1}$ of the polycarbonate (p=0.012) in an unpaired t-test (Figure 3). Between the polycarbonate and the fine mesh no difference was observed (p=0.12). Therefore, the rough mesh was selected for the remaining experiments in this study.

3.2 Reproducibility of the Algadisk reactor

The reproducibility of the lab-scale Algadisk reactor was evaluated by comparing the productivity of the disks at four different positions within the container (Figure 1). Productivity was monitored during four growth-harvest cycles for the same material (rough steel mesh) at a constant rotation speed of 11 rpm and 422 µmol $(m^2\ s)^{-1}$ light. Nutrients and CO_2 were supplied in excess. From Table I, it can be ascertained that disk 1 had significantly less productivity, less biomass thickness, and a higher mass fraction biomass to water when compared to disks 2, 3 and 4. That decrease was less pronounced for the biomass yield on light. Disks 2, 3 and 4 showed similar results. Neglecting the results of Disk 1, the average biomass productivity over the disks was 20.1 ±0.7 g $(m^2\ d)^{-1}$, and the average biomass yield in light was 0.88 ±0.04 g mol^{-1}.

3.3 Influence of disk rotation on productivity

The effect of various disk rotation speeds on productivity was evaluated by comparing rotation speeds of 3, 6, 11, and 20 rpm. This experiment was performed with disks of rough steel mesh at 422 µmol $(m^2\ s)^{-1}$ and under nutrient- and CO_2- replete conditions. The difference in

productivity between the different rotation speeds was minimal (Table II). The disk operated at 11 rpm, however, achieved significantly greater productivity than it did at 3 rpm (p 0.006) and at 20 rpm (p 0.002). The mass fraction of biomass to water and the biofilm thickness data did not exhibit a particular trend.

3.4 Substrate limitation

The influence of CO_2 limitation was evaluated for rotation speeds: 3, 11 and 20 rpm. This experiment was performed with disks of rough steel mesh at 422 µmol $(m^2\ s)^{-1}$. The CO_2 replete conditions (discussed in section 3.3) were compared to two CO_2 limiting conditions, resulting in 3 experimental conditions per rotation speed: (1) 15 mol m^{-3} CO_2 ($n \geq 8$ see section 3.3); (2) 0.7 mol m^{-3} CO_2 (n=8); and (3) 0.06 mol m^{-3} CO_2 (n=4) .

Comparing CO_2 replete conditions to CO_2 limiting conditions, we observed a significant decrease in productivity from 20 g $(m^2\ d)^{-1}$ to below 4 g $(m^2\ d)^{-1}$ (Figure 4A). The difference between 0.7 mol m^{-3} CO_2 and 0.06 mol m^{-3} CO_2 was more moderate, but still significant. For 0.06 mol m^{-3} CO_2, the different tested rotation speeds did not result in changed productivity (Figure 4A). In contrast, for 0.7 mol m^{-3} CO_2 the productivity of 3 rpm significantly differs from both 11 rpm (p=0.018) and 20 rpm (p=0.010). These results indicate that rotation speed influences the amount of substrate diffusing from the liquid phase into the biofilm. Between 11 rpm and 20 rpm, no significant difference was ascertained.

The mass fraction of biomass to water in the wet biofilm decreased with diminishing CO_2 concentrations (Figure 4B). Replete conditions led to a significantly greater mass fraction of biomass to water compared to 0.7 mol m^{-3} CO_2 ($p<0.001$) for all three tested rotation speeds. The data at 0.06 mol m^{-3} CO_2 exhibited a greater standard deviation and were not significantly different. From Figure 4B, however, a trend toward decreasing mass fraction of biomass to water in the wet biofilm could be detected with increasing CO_2 limitation.

3.5 Long-term stability

To perform the experiments, the Algadisk reactor was operated for 21 consecutive weeks. Due to technical problems, only the results corresponding to 13 weeks were incorporated into the experiments already discussed. The technical problems included: overnight pH rise to pH 10, 24 hours of darkness, and temperatures above 40 °C. These stressful conditions negatively influenced the productivity in the corresponding 7 day growth-harvest cycle. Productivities, however, recovered to maximal within one week after the conditions were reverted back to optimal. Furthermore, reproducibility was tested at weeks 5, 6, 7 and 19 to ensure no long-term changes occurred during the experiment (section 3.2). Although the experimental set-up was open no contaminations with grazers, other microalgae species or large increases in bacteria population where observed with microscope analysis. Figure 5 shows in chronological order the average productivity over all four disks per growth-harvest cycle.

4 Discussion

This study demonstrates that it is feasible to achieve consistent high disk surface productivities of 20 g $(m^2\ d)^{-1}$ over a period of 21 weeks (approximately 150 days) in the Algadisk system. Considering that, in the Algadisk system, only 58% of the disk surface was illuminated, the productivity based on illuminated surface is 34.7±1.3 g $(m^2\ d)^{-1}$. The productivity achieved in this study is in accordance to, or improved over, biofilm productivities described in literature (Table III).

Biomass yield on light and biomass productivities per ground surface are, collectively, an effective manner to evaluate systems' performances (Wijffels and Barbosa 2010). In lab-scale experiments, light is often manipulated, and possibly ground surface is not known or not representative for a potential large scale reactor. Biomass yield on light therefore is a more suitable manner to evaluate reactor performance. In our experiments, a biomass yield on light of 0.88 g mol^{-1} was achieved (Table II). This biomass yield on light is calculated based on the illuminated disk surface and productivity (Equation 2) and compared to values reported for

other biofilm-photobioreactors (Table III). The two systems that exploited light of 100 µmol (m^2 s)$^{-1}$ in their experiments, obtained lower productivities but achieved similar biomass yields on light as we did. Compared to lab-scale suspended systems our obtained biomass yield on light are in the higher range (Kliphuis et al. 2010; Takache et al. 2010), and approximately 2/3 of the theoretical maximum biomass yield on light of 1.5 g mol^{-1} (Blanken et al. 2013). As the biofilm in the Algadisk reactor is operated as a sequential batch, light is wasted after harvesting at the beginning of a new batch (Figure 2). By minimizing this loss of light, our biomass yield on light could be further improved. Furthermore future experiments have to validate that the obtained productivity and biomass yield on light can be maintained under outdoor light regimes. Although the obtained results are a good starting point for further scale-up.

During the experiments, biomass concentration in the suspension remained rather low (optical density measured at 750 nm remained below 1.0) although some biomass appeared to sediment at the bottom of the container. It was assumed that re-attachment of microalgae from the liquid to the disks did not occur. Due to the directional light source and the opaque container walls, the light intensity in the liquid was less than the light compensation point of photosynthesis (10 µmol (m^2 s)$^{-1}$) (Takache et al. 2010; Vejrazka et al. 2013). Light intensities lower than the light compensation point are too low to sustain growth. Therefore, it is most likely that most of the settled biomass came from the disks and that suspended growth of microalgae did not occur. The actual amount of settled biomass could not be measured. However, by preventing sedimentation of this biomass or by regularly harvesting the sediment, the productivity of the Algadisk could be further increased.

The harvested biomass from the lab-scale Algadisk reactor exhibited a high mass fraction biomass to water. The mass fraction biomass to water under CO_2 replete conditions was approximately 170 g kg^{-1} while it decreased to 120 g kg^{-1} under CO_2 limiting conditions. Mass fraction biomass to water in suspended systems is typically around 1 to 10 g kg^{-1} (Norsker et al.

2011). To concentrate the microalgae broth to a 150-250 g kg^{-1} mass fraction biomass to water, a broad spectrum of processes is proposed including: flocculation, flotation, filtration, and/or centrifugation (Pahl et al. 2013). The primary disadvantages of these processes are that they are energy consuming, species specific, and often difficult to scale (Pahl et al. 2013). Cultivation of microalgae in the Algadisk system would prevent the concentration issue and result in a cost and space reduction for downstream processing.

4.1 Evaluation of different disk materials

Previous studies comparing substratum for phototrophic biofilm growth are limited. One study indicated that *Chlorella* has an elevated attachment to polystyrene foam (Johnson and Wen 2010). Two other studies ascertained that cotton duct (Gross et al. 2013) and cotton rope (Christenson and Sims 2012) were the most favourable substratum for biofilm growth. These studies share the conclusion that structured surfaces promotes stable re-growth. This conclusion is in accordance with our findings that the more structured rough mesh exhibited greater and more consistent biofilm productivities. In our case, however, we could not determine the optimal pore depth since the rough mesh had the deepest pores.

The polycarbonate disk did not perform effectively, and productivity varied from one growth-harvest cycle to the other resulting in a greater standard deviation of the average productivity (Figure 3). The substantial standard deviation could be the result of lack of structure resulting in the formation of empty spots following harvesting which were required to be re-colonized by microalgae. Although re-growth was not stable, the initial attachment was the fastest for the polycarbonate disk (data not shown). This demonstrates the potential of the positively charged polyelectrolyte multilayer coating to improve initial attachment. However, Most important remains stable re-growth and robustness of the system.

4.2 Influence of disk rotation on productivity

During the experiment evaluating the influence of disk rotation on productivity, the differences were only minimal, although 11 rpm had a significantly greater productivity compared to 3 and 20 rpm. Based on traditional RBC literature, this could be due to the build-up of toxic compounds inside the biofilm at low rotation speeds and shear stress at high rotation speeds (Lu et al. 1997). However, the low effect of rotation speed on productivity shows a clear possibility to use larger disks in scaled up systems, e.g., based on the range of tested velocities (0.01 to 0.25 m/s) a disk with a diameter of 1.5 m could be used at 3 rpm.

Regarding the mass fraction of biomass to water and the biofilm thickness, no trend was observed during the various conditions assayed. This was contrary to other studies where biofilm surfaces exposed to increased hydrodynamic forces resulted in thinner and denser biofilms (Kugaprasatham et al. 1992; Picioreanu et al. 2000). This denser biofilm was observed in the reproducibility experiment for disk 1 which was exposed to liquid velocities of 2 m s^{-1} from the recycle inlet (Figure 1). The liquid velocity at the recycle inlet is much higher compared to the 0.01 to 0.25 m s^{-1} velocities that were applied when studying the influence of disk rotation on productivity (Table II). Although the biofilm on disk 1 grew more compact it still featured a lower productivity, which is most likely caused by hydrodynamic wash-off of microalgae. Another factor that might have influenced the mass fraction of biomass to water at lower rotation speeds could be that low rotation speeds resulted in a dryer biofilm. With low rotation speeds, the air/water frequency is also lower. To our knowledge there is no dedicated research performed on this topic, however, other researchers have noticed drying of the biofilm at low air/water frequencies (Gross et al. 2013).

4.3 Substrate limitation

For phototropic growth, CO_2 is the primary carbon source. If the CO_2 supply is less than CO_2 consumption, the productivity of the microalgae will decrease due to carbon limitation. During our experiments, a decrease in the CO_2 concentration resulted in a 5 to10 times reduction in

productivity compared to CO_2 replete conditions. The actual CO_2 concentrations in the bulk liquid were not measured, hence they remain unknown. From the operating conditions and assuming equilibrium between gas and liquid phases, we could estimate the maximal CO_2 concentration in the liquid as is described in the results section. In reality, however, equilibrium will not be achieved due to consumption of CO_2 by the microalgae and, therefore, the actual CO_2 concentrations will be lower.

The CO_2 dissolved in the bulk liquid is transported by diffusion into the biofilm. The rate of diffusion primarily depends on: concentration difference between bulk liquid and biofilm, distance over which diffusion occurs, and the diffusion coefficient. In the lab-scale Algadisk system, three factors play a role when cultivating microalgae under CO_2 limitation: (1) thickness of the stagnant layer between the biofilm and the bulk liquid or gas; (2) diffusion of dissolved CO_2 from the bulk liquid into the biofilm when it is submerged; and (3) diffusion of atmospheric CO_2 gas into the biofilm when it is above the water.

At 0.06 mol m^{-3} CO_2 no difference between the various rotation speeds was detected. This could indicate that the thickness of the stagnant film layer in the gas phase has only minimal influence on the diffusion of CO_2 to the biofilm, or it could indicate that the film layer covering the biofilm in the gas phase is not influenced by the rotation speed. The latter, however, is unlikely as a previous study has demonstrated a correlation between rotation speed and attached film thickness (Kubsad et al. 2004). At 0.7 mol m^{-3} CO_2, it seems that higher productivities are obtained with increasing rotation speeds. This could be due to improved mass transfer by a decreased stagnant film layer thickness in the liquid. More likely, however, is that the higher frequency between substrate absorption (biofilm submerged and dark) and substrate consumption (biofilm in air and illuminated) resulted in increased CO_2 uptake by the biofilm. During substrate limiting growth, the driving force for CO_2 diffusion into the biofilm is greatest upon re-entering the liquid as CO_2 concentration in the biofilm is at its lowest.

The above discussion illustrates that the absorption and consumption cycles introduced by growing a biofilm on a rotating disk are difficult to evaluate and that there is still opportunity for improvement upon better comprehension of these processes. Finally, it is noteworthy that the supply of sufficient nutrients is important to maintain optimal productivity. Therefore, nutrient supply should be carefully considered in the design of a scaled up Algadisk system.

5 Conclusions

In this study, *Chlorella sorokiniana* was cultivated in the Algadisk system. In the lab-scale RBC based photobioreactor, a productivity of 20.1 ±0.7 gram per m^2 disk surface per day and a biomass yield on light of 0.88 ±0.04 grams dry biomass per mol photons were achieved. The results obtained were stable over 21 weeks and showed that disk diameters up to 1.5 meter were possible. Together, the obtained results demonstrate a clear opportunity for larger scale Algadisk photobioreactors to produce microalgae biomass, although, adequate CO_2 supply should be ensured.

6 References

Blanken W, Cuaresma M, Wijffels RH, Janssen M. 2013. Cultivation of microalgae on artificial light comes at a cost. Algal Research 2(4):333-340.

Boelee NA, Temmink H, Janssen M, Buisman CJN, Wijffels RH. 2012. Scenario Analysis of Nutrient Removal from Municipal Wastewater by Microalgal Biofilms. Water 4(2):13.

Christenson LB, Sims RC. 2012. Rotating algal biofilm reactor and spool harvester for wastewater treatment with biofuels by-products. Biotechnol Bioeng 109(7):1674-84.

de Godos I, Gonzalez C, Becares E, Garcia-Encina PA, Munoz R. 2009. Simultaneous nutrients and carbon removal during pretreated swine slurry degradation in a tubular biofilm photobioreactor. Appl Microbiol Biotechnol 82(1):187-94.

Gross M, Henry W, Michael C, Wen Z. 2013. Development of a rotating algal biofilm growth system for attached microalgae growth with in situ biomass harvest. Bioresour Technol 150C:195-201.

Jacobsen A, Grahl-Nielsen O, Magnesen T. 2010. Does a large-scale continuous algal production system provide a stable supply of fatty acids to bivalve hatcheries? Journal of Applied Phycology 22(6):769-777.

Ji B, Zhang W, Zhang N, Wang J, Lutzu GA, Liu T. 2013a. Biofilm cultivation of the oleaginous microalgae Pseudochlorococcum sp. Bioprocess Biosyst Eng.

Ji C, Wang J, Zhang W, Liu J, Wang H, Gao L, Liu T. 2013b. An applicable nitrogen supply strategy for attached cultivation of Aucutodesmus obliquus. Journal of Applied Phycology.

Johnson MB, Wen Z. 2010. Development of an attached microalgal growth system for biofuel production. Appl Microbiol Biotechnol 85(3):525-34.

Kliphuis AMJ, Winter L, vejrazka C, Martens DE, Janssen M, Wijffels RH. 2010. Photosynthetic efficiency of Chlorella sorokiniana in a turbulently mixed short light-path photobioreactor. Biotechnology Progress 26(3):9.

Kubsad V, Chaudhari S, Gupta SK. 2004. Model for oxygen transfer in rotating biological contactor. Water Res 38(20):4297-304.

Kugaprasatham S, Nagaoka H, Ohgaki S. 1992. Effect of turbulence on nitrifying biofilms at non-limiting substrate conditions. Water Res 26(12):1629-1638.

Lu C, Li H-C, Lee LY, Lin M-R. 1997. Effects of disc rotational speed and submergence on the performance of an anaerobic rotating biological contactor. Environment International 23(2):253-263.

Naumann T, Çebi Z, Podola B, Melkonian M. 2012. Growing microalgae as aquaculture feeds on twin-layers: a novel solid-state photobioreactor. Journal of Applied Phycology 25(5):1413-1420.

Norsker NH, Barbosa MJ, Vermue MH, Wijffels RH. 2011. Microalgal production--a close look at the economics. Biotechnol Adv 29(1):24-7.

Nowack EC, Podola B, Melkonian M. 2005. The 96-well twin-layer system: a novel approach in the cultivation of microalgae. Protist 156(2):239-51.

Orandi S, Lewis DM, Moheimani NR. 2012. Biofilm establishment and heavy metal removal capacity of an indigenous mining algal-microbial consortium in a photo-rotating biological contactor. J Ind Microbiol Biotechnol 39(9):1321-31.

Ozkan A, Kinney K, Katz L, Berberoglu H. 2012. Reduction of water and energy requirement of algae cultivation using an algae biofilm photobioreactor. Bioresour Technol 114:542-8.

Pahl SL, Lee AK, Kalaitzidis T, Ashman PJ, Sathe S, Lewis DM. 2013. Harvesting, Thickening and Dewatering Microalgae Biomass.165-185.

Patwardhan AW. 2003. Rotating Biological Contactors: A Review. Industrial & Engineering Chemistry Research 42(10):2035-2051.

Picioreanu C, van Loosdrecht MCM, Heijnen JJ. 2000. A theoretical study on the effect of surface roughness on mass transport and transformation in biofilms. Biotechnol Bioeng 68(4):355-369.

Salim S, Gilissen L, Rinzema A, Vermue MH, Wijffels RH. 2013. Modeling microalgal flocculation and sedimentation. Bioresour Technol 144:602-7.

Shi J, Podola B, Melkonian M. 2007. Removal of nitrogen and phosphorus from wastewater using microalgae immobilized on twin layers: an experimental study. Journal of Applied Phycology 19(5):417-423.

Sorokin C, Myers J. 1953. A high-temperature strain of *Chlorella*. Science 117(3039):330-331.

Takache H, Christophe G, Cornet J-F, Pruvost J. 2010. Experimental and theoretical assessment of maximum productivities for the microalgae *Chlamydomonas reinhardtii* in two different geometries of photobioreactors. Biotechnology Progress 26(2):431-440.

Vejrazka C, Janssen M, Benvenuti G, Streefland M, Wijffels RH. 2013. Photosynthetic efficiency and oxygen evolution of Chlamydomonas reinhardtii under continuous and flashing light. Appl Microbiol Biotechnol 97(4):1523-32.

Wei Q, Hu Z, Li G, Xiao B, Sun H, Tao M. 2008. Removing nitrogen and phosphorus from simulated wastewater using algal biofilm technique. Frontiers of Environmental Science & Engineering in China 2(4):446-451.

Wijffels RH, Barbosa MJ. 2010. An outlook on microalgal biofuels. Science 329(5993):796-9.

Wilkie AC, Mulbry W. 2002. Recovery of dairy manure nutrients by benthic freshwater algae. Bioresour Technol 84(1):10.

Wolf G, Picioreanu C, van Loosdrecht MC. 2007. Kinetic modeling of phototrophic biofilms: the PHOBIA model. Biotechnol Bioeng 97(5):1064-79.

The authors would like to thank Luisaldo Sandate Flores for work performed in the lab and the Algadisk consortium for their participation in this manuscript. The research leading to these results has received funding from the European Union's Seventh Framework Programme (FP7/2007- 2013) - managed by REA Research Executive Agency - under grant agreement no. 286887. Currently S. Libor works for OLAJGÉP-TEC (a company within the Algadisk consortium).

Appendices

A. light distribution over the disk

Figure A.1. Different measure positions on the disk surface, with hole 3 as the centre of the disk.

Table A.1. Light distribution over the different disk positions with F for front and B for Back.

Light is measured in μmol $(m^2\ s)^{-1}$.

	disk 1 F	disk 1 B	disk 2 F	disk 2 B	disk 3 F	disk 3 B	disk 4 F	disk 4 B
1	324 ± 18	309 ± 16	322 ± 32	329 ± 12	335 ± 10	330 ± 15	331 ± 40	304 ± 28
2	447 ± 26	420 ± 27	453 ± 36	443 ± 16	470 ± 20	442 ± 12	462 ± 22	393 ± 23
3	498 ± 22	447 ± 43	508 ± 20	463 ± 20	531 ± 36	465 ± 10	511 ± 14	433 ± 22
4	437 ± 8	416 ± 31	421 ± 18	441 ± 25	452 ± 32	417 ± 19	459 ± 19	395 ± 19
5	318 ± 15	305 ± 13	312 ± 14	331 ± 16	329 ± 28	307 ± 37	316 ± 5	302 ± 33
6	448 ± 38	409 ± 41	448 ± 37	405 ± 20	471 ± 19	425 ± 12	448 ± 36	388 ± 24
7	602 ± 49	548 ± 47	599 ± 54	541 ± 37	637 ± 48	567 ± 9	631 ± 25	502 ± 13
8	589 ± 33	543 ± 56	519 ± 68	542 ± 35	618 ± 54	551 ± 23	632 ± 26	506 ± 24
9	433 ± 11	424 ± 38	449 ± 27	420 ± 18	453 ± 49	410 ± 36	450 ± 12	397 ± 39
10	474 ± 42	430 ± 33	455 ± 44	423 ± 26	458 ± 57	449 ± 6	472 ± 31	400 ± 10
11	518 ± 25	497 ± 49	527 ± 47	491 ± 36	582 ± 58	508 ± 19	560 ± 31	460 ± 16
12	458 ± 8	438 ± 41	446 ± 38	437 ± 23	483 ± 46	443 ± 27	480 ± 26	408 ± 26
ave	462 ± 17	432 ± 33	455 ± 22	439 ± 21	485 ± 35	443 ± 11	479 ± 16	407 ± 18

Figure 1. Schematic overview of Algadisk lab scale reactor. D = disk, M = motor driving the disk, C = container , T = temperature control system, BT = buffer tank. Both the top of the container and buffer tank are open. Liquid in the reactor vessel flows from left to right, and the direction of disk rotation is depicted in the figure.

Figure 2. Photographs taken during a typical 7 day growth-harvest cycle on the rough metal mesh. The day within the growth-harvest cycle is indicated in white. On day 7, biofilm is harvested and a new cycle begins.

Figure 3. Average productivity over 4 growth-harvest cycles with 8 measurements per disk (4 weeks times 2 disk sides) for three types of disk materials. The experiment was performed under light limited conditions at a constant rotation speed of 11 rpm. Error bars indicate the standard deviation.

Figure 4. Average productivity (A) and Mass fraction of biomass to water in wet biofilm (B) for different CO_2 concentrations at three rotation speeds. The experiment with 15 mol m^{-3} CO_2 was at light limiting and nutrient replete conditions. For 0.7 mol m^{-3} CO_2, the bulk liquid in the buffer tank was continuously gassed with 0.5 $\%_{v/v}$ CO_2 enriched air. For 0.06 mol m^{-3} CO_2, the bulk liquid was not gassed and thus there was only atmospheric CO_2 available via direct gas biofilm contact. The error bars indicate the standard deviation.

Figure 5. Average productivity, calculated as the average of the 4 disks productivity per growth-harvest cycle, in chronological order. The grey bars represent the growth-harvest cycles that were not employed due to technical problems. The white bars represent the data from reproducibility experiment. The cross lined bars represent the experiments on rotation speed and

the dark dotted and light dotted represent the experiments on CO_2 limitation (dark dotted without sparging of the bulk liquid and light dotted with sparging of the bulk liquid).

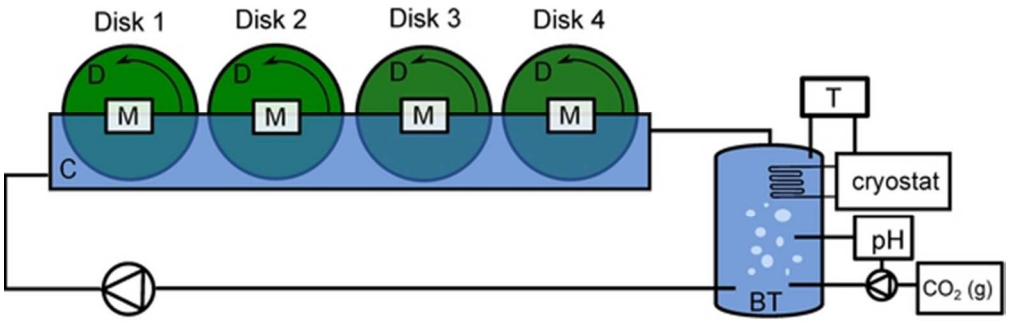

Figure 1. Schematic overview of Algadisk lab scale reactor. D = disk, M = motor driving the disk, C = container , T = temperature control system, BT = buffer tank. Both the top of the container and buffer tank are open. Liquid in the reactor vessel flows from left to right, and the direction of disk rotation is depicted in the figure.
50x15mm (300 x 300 DPI)

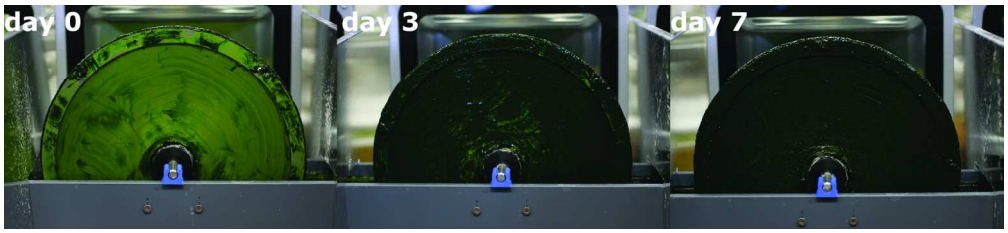

Figure 2. Photographs taken during a typical 7 day growth-harvest cycle on the rough metal mesh. The day within the growth-harvest cycle is indicated in white. On day 7, biofilm is harvested and a new cycle begins.
162x36mm (300 x 300 DPI)

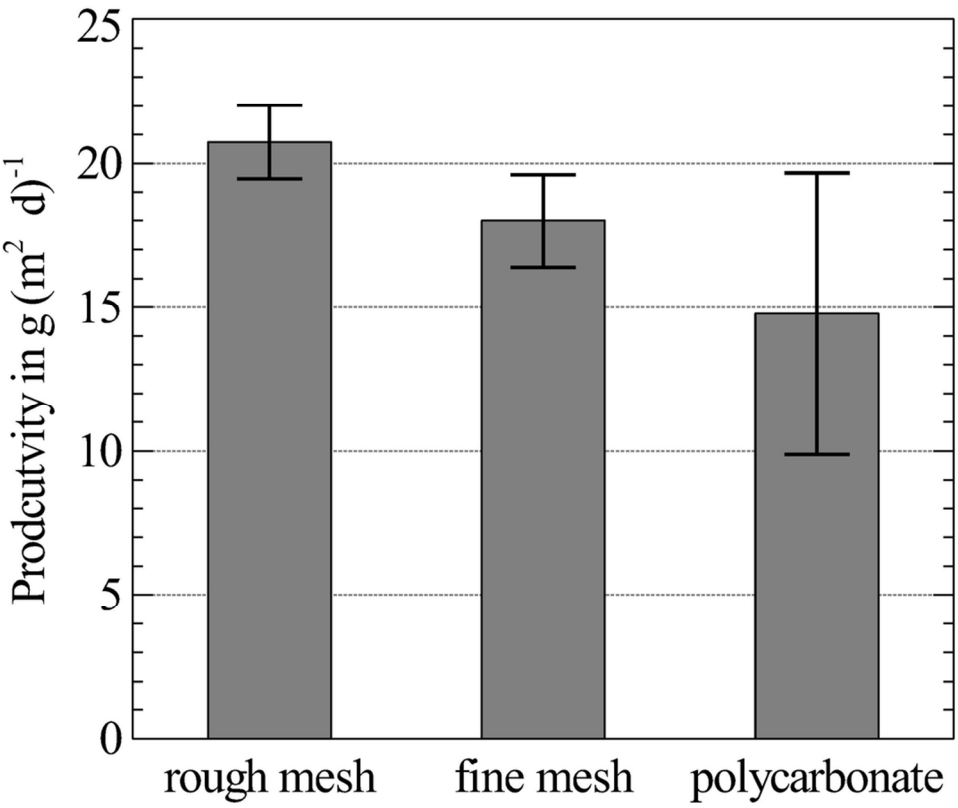

Figure 3. Average productivity over 4 growth-harvest cycles with 8 measurements per disk (4 weeks times 2 disk sides) for three types of disk materials. The experiment was performed under light limited conditions at a constant rotation speed of 11 rpm. Error bars indicate the standard deviation.
94x85mm (300 x 300 DPI)

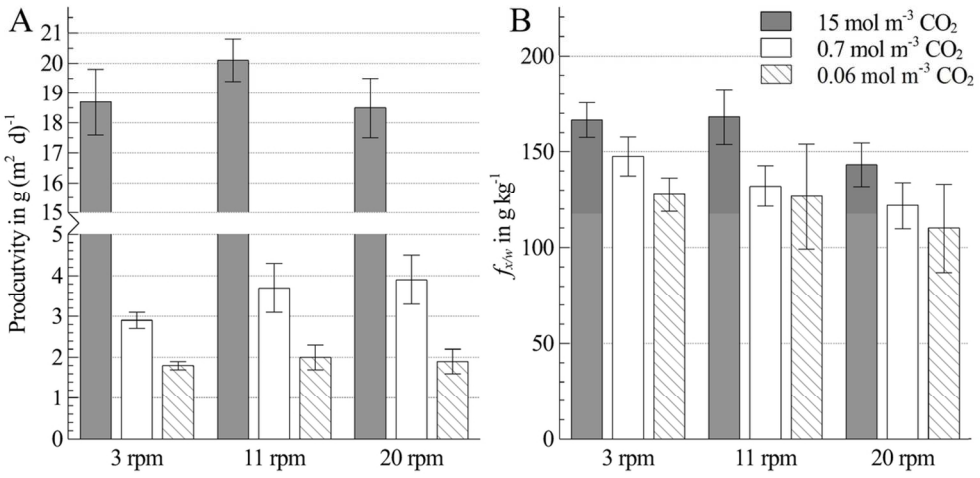

Figure 4. Average productivity (A) and Mass fraction of biomass to water in wet biofilm (B) for different CO_2 concentrations at three rotation speeds. The experiment with 15 mol m^{-3} $CO_2$was at light limiting and nutrient replete conditions. For 0.7 mol m^{-3} CO_2, the bulk liquid in the buffer tank was continuously gassed with 0.5 %v/v CO_2enriched air. For 0.06 mol m^{-3} CO_2, the bulk liquid was not gassed and thus there was only atmospheric CO_2available via direct gas biofilm contact. The error bars indicate the standard deviation.
108x55mm (300 x 300 DPI)

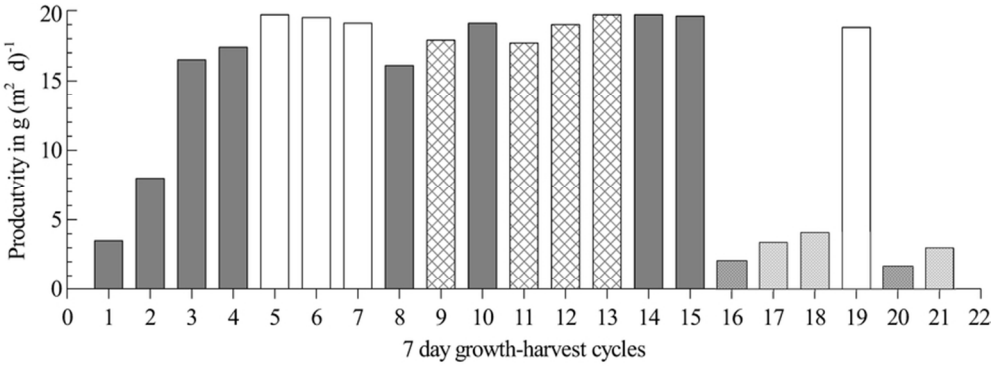

Figure 5. Average productivity, calculated as the average of the 4 disks productivity per growth-harvest cycle, in chronological order. The grey bars represent the growth-harvest cycles that were not employed due to technical problems. The white bars represent the data from reproducibility experiment. The cross lined bars represent the experiments on rotation speed and the dark dotted and light dotted represent the experiments on CO_2 limitation (dark dotted without sparging of the bulk liquid and light dotted with sparging of the bulk liquid).
79x29mm (300 x 300 DPI)

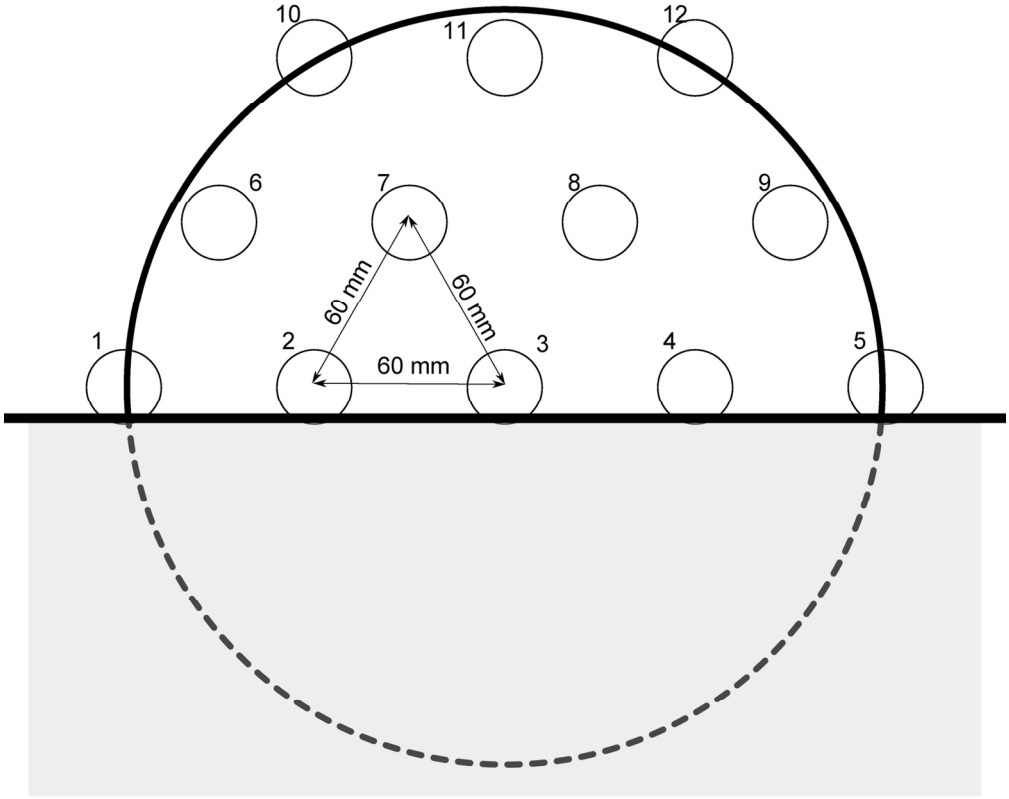

Figure A.1. Different measure positions on the disk surface, with hole 3 as the centre of the disk.
141x112mm (300 x 300 DPI)

Table I. The surface productivity (P_x), mass fraction biomass to water ($f_{x/w}$), biomass yield to light ($Y_{x/ph}$) and biofilm thickness (z) results of the reproducibility experiment. The reproducibility experiment is performed at nutrient replete conditions with a light intensity of 422 µmol $(m^2\ s)^{-1}$ on a rough metal mesh at a constant rotation speed of 11 rpm. Parameter 'n' represents the number of experiments. Each experiment represents data of one side of the disk during a 7 day growth-harvest cycle. Standard deviation is shown.

	P_x $g\ (m^2\ d)^{-1}$	$f_{x/w}$ $g\ kg^{-1}$	$Y_{x/ph}$ $g\ mol^{-1}$	z μm	n
disk 1	17.5 ±2.1	192 ±6	0,77 ±0,10	634 ±76	8
disk 2	19.9 ±0,8*	174 ±9**	0,89 ±0,06*	800 ±41**	8
disk 3	19,8 ±0,2*	173 ±4**	0,85 ±0,06	797 ±24**	6
disk 4	20,1 ±0,7**	172 ±9**	0,91 ±0,09*	847 ±67**	8

* $p<0.05$ with unpaired t-test compared to disk 1

** $p<0.01$ with unpaired t-test compared to disk 1

Table II. The surface productivity (P_x), mass fraction biomass to water ($f_{x/w}$), biomass yield to light ($Y_{x/ph}$), biofilm thickness (z) results and disk velocity for different rotation speeds. The disk velocity provides the lowest and highest liquid velocity corresponding to that revolution per minute. Experiments are performed in nutrient replete conditions with a light intensity of 422 µmol $(m^2\ s)^{-1}$ on a rough steel mesh. Parameter 'n' represents the number of experiments. Each experiment represents data for one disk side during a 7 day growth-harvest cycle.

	P_x	$f_{x/w}$	z	n	disk velocity	
					low	high
	$g\ (m^2\ d)^{-1}$	$g\ kg^{-1}$	μm	#	$m\ s^{-1}$	$m\ s^{-1}$
3 rpm	18.7 ±1.1	166 ±9	783 ±60	8	0.008	0.038
6 rpm	19.5 ±1.3	152 ±13	900 ±138	6	0.016	0.075
11 rpm	20.1 ±0.7	168 ±15	842 ±101	24	0.029	0.138
20 rpm	18.5 ±1.0	143 ±11	910 ±113	8	0.052	0.251

Table III. Comparison between biofilm reactors reported in literature and this study for biomass productivity (P_X), biomass yield on light ($Y_{X/e}$) and light conditions. If a day/night cycle is applied the light intensities depicted are averaged over 24 hours (thus include the dark). For some studies to a biomass yield on light could not be calculated.

P_X	$Y_{X/e}$	Light intensity	L/D	Species	Literature
$g\ (m^2\ d)^{-1}$	$g\ mol^{-1}$	$\mu mol\ (m^2\ s)^{-1}$	h/h		
20	0.9	422	24/0	*C. Sorokinana*	This study
6	1.0	96	24/0	*Pseudochlorococcum*	Ji et al. 2013a
9	1.1	100	24/0	*A. obliquus*	Ji et al. 2013b
14	-	642	15/9*	*C. vulgaris*	Gross et al. 2013
20-31	-	208	12/12*	Mixed culture	Christenson and Sims 2012
2	-	18-320	15/9*	*Phaeodactylum*	Naumann et al. 2012

* Actual day-length varies due to seasonal changes